1-1-2010

Automatic parameter selection for feature-enhanced radar image restoration

Moeness G Amin
Villanova University, mamin@uow.edu.au

Cher Hau Seng
University of Wollongong, aseng@uow.edu.au

Son Lam Phung
University of Wollongong, phung@uow.edu.au

Abdesselam Bouzerdoum
University of Wollongong, bouzer@uow.edu.au

Automatic parameter selection for feature-enhanced radar image restoration

Abstract

In this paper, we propose a new technique for optimum parameter selection in non-quadratic radar image restoration. Although both the regularization hyper-parameter and the norm value are influential factors in the characteristics of the formed restoration, most existing optimization methods either require memory intensive computation or prior knowledge of the noise. Here, we present a contrast measure-based method for automated hyper-parameter selection. The proposed method is then extended to optimize the norm value used in non-quadratic image formation and restoration. The proposed method is evaluated on the MSTAR public target database and compared to the GCV method. Experimental results show that the proposed method yields better image quality at a much reduced computational cost.

Keywords

image, radar, enhanced, feature, selection, automatic, restoration, parameter

Disciplines

Physical Sciences and Mathematics

Publication Details

Seng, C., Bouzerdoum, A., Phung, S. & Amin, M. (2010). Automatic parameter selection for feature-enhanced radar image restoration. 2010 IEEE Radar Conference (pp. 001123-001127). USA: IEEE.

Automatic Parameter Selection for Feature-Enhanced Radar Image Restoration

C. H. Seng, A. Bouzerdoum and S. L. Phung
School of Electrical, Computer and Telecommunications Engineering
University of Wollongong, Wollongong, NSW 2522, Australia
Email: {aseng, a.bouzerdoum, phung}@uow.edu.au

M. Amin
Centre for Advanced Communications
Villanova University, Villanova, PA 19085, USA
Email: moeness.amin@villanova.edu

***Abstract*—In this paper, we propose a new technique for optimum parameter selection in non-quadratic radar image restoration. Although both the regularization *hyper-parameter* and the norm value are influential factors in the characteristics of the formed restoration, most existing optimization methods either require memory intensive computation or prior knowledge of the noise. Here, we present a contrast measure-based method for automated hyper-parameter selection. The proposed method is then extended to optimize the norm value used in non-quadratic image formation and restoration. The proposed method is evaluated on the MSTAR public target database and compared to the GCV method. Experimental results show that the proposed method yields better image quality at a much reduced computational cost.**

I. Introduction

The radar image formation process is usually corrupted by noise and other interferences. Generally, the radar image observation can be formulated as follows:

$$\mathbf{g} = \mathbf{T}\mathbf{f} + \mathbf{w}, \tag{1}$$

where $\mathbf{g}$ is the observed data, $\mathbf{f}$ is the ideal image, $\mathbf{T}$ is the transformation matrix specific to the radar device and $\mathbf{w}$ represents additive noise [1], [2]. As image restoration is an ill-posed inverse problem, regularization methods are introduced to obtain solutions that are stable in the presence of perturbations [3].

Regularization methods for image restoration include prior information about the field, $\mathbf{f}$, to constrain the solution, and hence avoiding noise amplifications. The restoration problem can then be expressed as

$$\hat{\mathbf{f}} = \arg\min_{\mathbf{f}}\{||\mathbf{g} - \mathbf{T}\mathbf{f}||_2^2 + \lambda^2\ \psi(\mathbf{f})\}, \tag{2}$$

where the first term is a data fidelity term that incorporates the image acquisition observation model, $\psi(\mathbf{f})$ is the regularizer or side constraint, which is used to stabilize the solution in the presence of interferences and λ is a non-negative scalar parameter that is used to control the trade-off between the data fidelity term and the regularizer to yield a system of approximate solutions, $\hat{\mathbf{f}}(\lambda)$, that are stable.

The most commonly used regularization method is the Tikhonov approach, and its side constraint is given as

$$\psi(\mathbf{f}) = ||\mathbf{D}\mathbf{f}||_2^2, \tag{3}$$

This work is supported by a grant from the Australian Research Council.

where $\mathbf{D}$ is an image operator and $||\cdot||_2$ denotes the l_2-norm. Although the use of the quadratic l_2-based criteria is desirable for its linearity, such linear filters tend to blur details in the restoration when used to suppress the effect of high-frequency noise [2]. Therefore, a more generalized approach is considered by introducing a non-quadratic criteria for the regularizer. The side constraint is now rewritten as

$$\psi(\mathbf{f}) = ||\mathbf{D}\mathbf{f}||_p^p, \tag{4}$$

where $||\cdot||_p^p$ denotes the l_p-norm raised to the power p.

For feature-enhanced restorations, common choices for image operator $\mathbf{D}$ are identity matrices, $\mathbf{I}$, and 2-D derivative operators, usually represented by the gradient ∇ [4]. Cetin and Karl [5] suggested that the side constraint function, $||\mathbf{f}||_p^p$ with $p \leq 1$, enhances point-based features and improves the resolvability of objects when there is a small number of dominant scatterers in the scene. In comparison, the function, $||\nabla\mathbf{f}||_p^p$ with $p \approx 1$, enhances region-based shape features that are useful for segmenting the object, shadow and background regions.

Smoothing approximations were also introduced to the side constraint in (4) to avoid non-differentiability problems associated with the objective function when l_p-norms of $p < 1$ are used. The regularizer now takes the following form [6]:

$$\psi(\mathbf{f}) = \sum_{i=1}^{N}[|(\mathbf{D}\mathbf{f})_i|^2 + \varepsilon]^{p/2}, \tag{5}$$

where N represents the length of the complex vector $\mathbf{D}\mathbf{f}$, $(\mathbf{x})_\mathbf{i}$ denotes the i-th element of $\mathbf{x}$, and ε is a small positive constant. Equation (2) with side constraint (5) can then be efficiently solved using an iterative method that is based on half-quadratic regularization [5].

Besides an efficient iterative method, the restoration also requires an optimum choice of the scalar parameter λ, known as the *regularization parameter* or *hyper-parameter*, to balance the fidelity of data and prior knowledge. However, a small regularization parameter value will produce an under-regularized restoration that is dominated by large, high-frequency noise components. On the other hand, large values of λ will over-regularize by imposing greater importance on the regularizer, causing important information to be lost. Therefore, a balanced choice of this parameter is important in regularization methods.

978-1-4244-5813-4/10/$26.00 ©2010 IEEE

In this paper, we introduce an automatic parameter selection technique that is suitable for radar image restoration. The remainder of the paper is organized as follows. Section II presents the proposed hyper-parameter selection method, and Section III describes an extension of the method for norm optimization. Section IV analyzes an application of the proposed method to the MSTAR public target data set, and Section V concludes the paper.

II. Hyper-Parameter Selection Methods

Existing methods for hyper-parameter selection include Visual Inspection, Discrepancy Principle, L-curve, Generalized Cross-Validation [2] and Hierarchical Bayesian methods [7]. However, the Visual Inspection method requires the presence of a human operator who has prior knowledge about the ideal image, while both the Discrepancy Principle and Hierarchical Bayesian methods require prior knowledge or estimates of the noise. In addition, both the L-curve and the Generalized Cross-Validation (GCV) methods mainly cater for continuous functions where l_p-norms with $p \geq 1$ are used.

Batu and Cetin [8] recently investigated automated hyper-parameter selection using the GCV method, by minimizing an objective function that caters for non-continuous functions, and was applied to SAR image formation. However, their proposed method suffers from computational difficulties that involve large-scale matrix multiplications and inversions. In this paper, we propose a hyper-parameter selection method that is computationally less intensive, while coping with non-continuous functions.

A. Image Quality Measure

A reliable image quality measure is required to search for an optimum hyper-parameter. However, most image quality assessment metrics require the presence of a reference image, which is usually not readily available in radar imaging. Besides, some metrics cannot be expressed in closed-form or are not suitable for combination with the optimization objective function. Therefore, we seek an image quality metric that doesn't require a reference image.

A common image quality assessment method that is used in a variety of radar imaging modalities, such as SAR [9], ISAR [10] and sonar [11], is the contrast measure. This metric has been used for radar autofocusing to determine the degree of smearing and blurring in formed images. Ahmad et al. [12] showed that images that were formed without errors tend to have a higher contrast than those formed with errors. Higher order metrics, such as the n-th standardized moments with $n > 3$, were also shown to be more sensitive to minor perturbations in the data.

Therefore, we propose to investigate the use of the fourth standardized moment, also known as the kurtosis, as our image quality measure to facilitate automated hyper-parameter selection. Instead of using the kurtosis for radar hardware autofocusing, it is now used as an image quality measure to tune and select the optimum hyper-parameter in regularized image restoration methods.

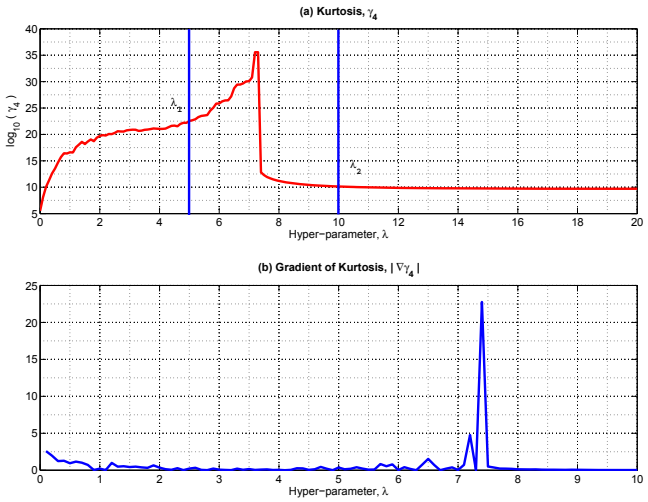

Fig. 1. (a) Kurtosis of the reconstructed image for $\lambda \in [0, 20]$. (b) The absolute gradient of the kurtosis, $|\nabla\gamma_4(\lambda)|$.

The kurtosis is defined as

$$\gamma_4 = \frac{\sum_{i=1}^{N}[\hat{f}_i - \hat{\mu}]^4}{(N-1)\hat{\sigma}^4}, \tag{6}$$

where N denotes the number of pixels and $\hat{f}_i$ denotes the i-th element of vector $\hat{\mathbf{f}}$. $\hat{\mu}$ and $\hat{\sigma}$ represent, respectively, the sample mean and the sample standard deviation of $\hat{\mathbf{f}}$:

$$\hat{\mu} = \frac{1}{N}\sum_{i=1}^{N}\hat{f}_i, \tag{7}$$

and

$$\hat{\sigma} = \left[\frac{1}{N-1}\sum_{i=1}^{N}(\hat{f}_i - \hat{\mu})^2\right]^{1/2}. \tag{8}$$

We first evaluate the kurtosis as a function of the hyper-parameter, $\lambda \geq 0$, on an interval $[a, b]$, with steps $\Delta\lambda$. Using an exhaustive search, the restoration, given in (2) with side constraint (5), is computed for all λ values within the interval $[a, b]$. At the end of each restoration, the kurtosis is used to determine the quality of the reconstructed image, $\hat{\mathbf{f}}(\lambda)$.

For comparison purposes, the Target-to-Clutter ratio (TCR) is also calculated at the end of each restoration. Commonly used for SAR imaging evaluations [13], the TCR measures the accentuation of the target pixels with respect to the background, and is defined as

$$TCR = 10log_{10}\left[\frac{\frac{1}{N_T}\sum_{(i,j)\in T}|\hat{\mathbf{f}}_{i,j}|^2}{\frac{1}{N_C}\sum_{(i,j)\in C}|\hat{\mathbf{f}}_{i,j}|^2}\right] \tag{9}$$

where $\hat{\mathbf{f}}_{i,j}$ is the ij-th element of the restored image, T denotes the predefined target region, C denotes the predefined clutter region, and N_T and N_C are the number of pixels in T and C, respectively.

Figure 1 shows the kurtosis curve for the restored images using $\lambda \in [0, 20]$, while Fig. 2 shows the restoration results for the range of λ values that produce a high kurtosis value.

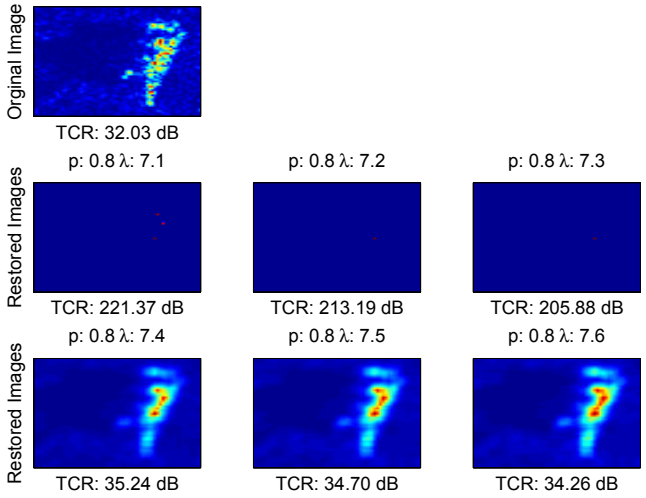

Fig. 2. Restored images for $l_{0.8}$-norm using different λ values, with their respective Target-to-Clutter ratios.

These preliminary results show that the optimum λ value will split the restorations into two distinct regions; one with high TCRs, but without much visual information, and the other with lower TCRs, but is visually more appealing and allows for object identification.

Empirical observations suggest that the hyper-parameter at this break point is the optimum value for the restorations, for any norm value. We probe for this optimum value by taking the absolute gradient of the kurtosis, where the maximum of the absolute gradient of the kurtosis will then correlate directly to the optimum hyper-parameter. An example is shown in Fig. 1 where the optimum λ is 7.4 for the $l_{0.8}$-norm.

Hence, the kurtosis is a suitable image quality measure that can be used to select the optimum hyper-parameter in feature-enhanced image restoration methods, where the hyper-parameter producing the best image quality is chosen as the optimum parameter.

Although some may argue that it is preferable to have a higher TCR value than a visually appealing image, we believe that restored images should have a visual appeal that could be easily discernable by a human operator who do not have prior knowledge about the target. This is because a simple thresholding could produce an image with a high TCR but low visual appeal.

B. Overview of the Proposed Method

Since the exhaustive search method yields extensive computations, we use the golden section search algorithm to probe for the optimum hyper-parameter value that produces the maximum kurtosis value (Fig. 1a). This search algorithm allows us to reduce the interval $[a, b]$ to a smaller range, $[a, \lambda_2]$ or $[\lambda_1, b]$. The restoration using λ_1 and λ_2 are evaluated and their kurtosis values, $\gamma_4(\lambda_1)$ and $\gamma_4(\lambda_2)$, are computed. The new interval is then determined as follows:

Case 1: If $\gamma_4(\lambda_1) > \gamma_4(\lambda_2)$, then the new interval is $[a, \lambda_2]$.
Case 2: If $\gamma_4(\lambda_1) \leq \gamma_4(\lambda_2)$, then the new interval is $[\lambda_1, b]$.

After determining the new interval, represented by $[a_1, b_1]$, the restoration is performed for all λ values within the interval. At the end of each restoration, the kurtosis value is computed for the reconstructed image, $\hat{\mathbf{f}}(\lambda)$. The λ value corresponding to the highest peak in the absolute gradient of the kurtosis is selected as the optimum parameter (refer to Fig. 1b).

The pseudo-code for the proposed method is presented below.

1) Define the interval $[a, b]$.
2) Using the golden section search, determine the new interval $[a_1, b_1]$.
3) Initialize $k = 0$ and $\lambda_0 = a_1$.
4) For $\lambda = \lambda_k$, compute the reconstructed image $\hat{\mathbf{f}}(\lambda_\mathbf{k})$.
5) Compute the kurtosis of $\hat{\mathbf{f}}(\lambda_\mathbf{k})$, $\gamma_4(\lambda_k)$.
6) Increment $k = k + 1$ and $\lambda_k = \lambda_k + \Delta\lambda$.
7) If $\lambda_k \leq b_1$, repeat Steps 4 to 6.
8) Compute the gradient of the kurtosis with respect to λ, $\nabla\gamma_4(\lambda)$.
9) Select the optimum hyper-parameter as λ_k that yields the maximum absolute value of the gradient:

$$\lambda^* = \arg\max_{\lambda} |\nabla\gamma_4(\lambda)|.$$

III. Extensions to Norm Optimization

In most regularization methods, the norm values of 1 and 2 are usually used. For instance, the l_1-norm is used for Total Variation Regularization and the l_2-norm is used for Tikhonov Regularization. In this section, we investigate the performance of other norm values with $p < 1$ and $1 < p < 2$ by extending the proposed method to optimize the norm values used for the restorations.

The norm values are first sampled over the interval $[0.2, 2]$. For every norm value, the corresponding peak of the absolute gradient of the kurtosis value, $\max|\nabla\gamma_4(\lambda)|_p$, that produce the optimum λ is recorded. A graph of $\max|\nabla\gamma_4(\lambda)|_p$ versus the norm, p is then plotted for all norm values within the interval.

Empirical observations show that the highest peak in the absolute value of the gradient of $\max|\nabla\gamma_4(\lambda)|_p$ correlates directly with the optimum norm value. For example, Fig. 3 shows that the optimum norm value for the restoration is 0.8.

IV. Experimental Results

We apply the proposed method to process SAR scenes from the Moving and Stationary Target Acquisition and Recognition (MSTAR) public target data set [14]. This database was collected using an X-band SAR sensor in one foot resolution and provides formed 128x128 imagery of a T-72 Main Battle Tank, a BTR-70 Armored Personnel Carrier, and a BMP2 Infantry Fighting Vehicle. In our experiments, we investigate the performance of the proposed hyper-parameter selection method against the GCV method on both point-based and region-based feature enhancements.

The norm value $p = 1$ is used for all the experiments as it was observed by Cetin and Karl [5] that for point-enhanced restorations, the side constraint function, $||\mathbf{f}||_p^p$ with $p \leq 1$, enhances point-based features and improves the resolvability

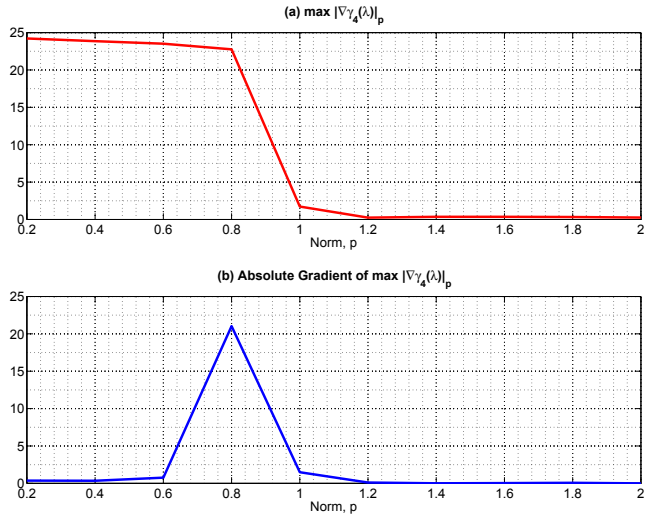

Fig. 3. (a) $\max|\nabla\gamma_4(\lambda)|_p$ for $p \in [0.2, 2]$. (b) The absolute gradient of $\max|\nabla\gamma_4(\lambda)|_p$.

of objects. Similarly for region-enhanced restorations, $||\nabla \mathbf{f}||_p^p$ with $p \approx 1$, enhances features that are useful for region segmentation. The interval for λ was initially set to $[0, 20]$, with a step size $\Delta\lambda = 0.1$. This interval is then reduced to $[0, 10]$ using the golden section search algorithm. In addition, a small value, $\varepsilon = 10^{-5}$, is also chosen for the smoothing constant to ensure that the behavior of the solution is not affected. The conjugate gradient method is then used to iteratively restore the images and the hyper-parameter shown in the results are automatically selected by the respective methods.

The experiments were then extended to norm optimization, where the norm values producing the best restoration are automatically selected by the proposed method.

A. Point-based Feature Enhancements

For point-based feature enhanced restorations, an identity matrix is chosen as the operator $\mathbf{D}$. Figure 4 shows the results for point-based enhancements with the l_1-norm, where automated hyper-parameter selection is evaluated. It can be observed that the proposed method provides a similar performance to the GCV method, but it is computationally less intensive.

Using norm values of p in $[0.2, 2]$, the proposed extension to norm optimization is evaluated for choosing the best parameter combination for the restoration. It is observed that a smaller norm value of $p = 0.8$ produces a better solution; it enhances the main body and the edges of the objects.

B. Region-based Feature Enhancements

The experiment was then repeated for region-based feature enhanced restorations, where a 2-D derivative operator, ∇ is chosen as the operator $\mathbf{D}$. The results for region-based enhancements with norm value of $p = 1$ is shown in Fig. 5. It can be observed that the GCV method failed to segment the regions, while the proposed method consistently enhances the region, separating the shape of the object, its shadow and the background.

The proposed norm optimization method was then evaluated for $p \in [0.2, 2]$. It can be observed that for this restoration, a higher norm value of 1.2 produces a sharper restoration.

V. Conclusion

We have presented a new approach for automated hyper-parameter selection that is based on contrast measures. We have also successfully extended the proposed method for norm optimization to investigate the performance of norm values of $p < 1$ and $1 < p < 2$. Experimental results based on the MSTAR public targets data set is also presented, which demonstrate the effectiveness of the proposed method on hyper-parameter selection and norm optimization for feature-enhanced radar image restoration. In conclusion, the proposed method generates reasonable parameter choices for radar image restoration. Furthermore, it is also computationally less intensive and is independent from prior knowledge of noise.

References

[1] M. Sezan and A. Tekalp, "Survey of recent developments in digital image restoration," *Optical Engineering*, vol. 29, no. 5, pp. 393–404, 1990.

[2] W. Karl, "Regularization in image restoration and reconstruction," in *Handbook of Image and Video Processing*, A. Bovik, Ed. Academic Press, 2000, pp. 141–160.

[3] G. Demoment, "Image reconstruction and restoration: Overview of common estimation structures and problems," *IEEE Transactions on Acoustics, Speech, and Signal Processing*, vol. 37, no. 12, pp. 2024–2036, 1989.

[4] M. Cetin, "Featured-enhanced synthetic aperture radar imaging," PhD dissertation, Boston University, 2001.

[5] M. Cetin and W. Karl, "Feature-enhanced synthetic aperture radar image formation based on nonquadratic regularization," *IEEE Transactions on Image Processing*, vol. 10, no. 4, pp. 623–631, 2001.

[6] C. Vogel and M. Oman, "Fast, robust total variation-based reconstruction of noisy, blurred images," *IEEE Transactions on Image Processing*, vol. 7, no. 6, pp. 813–824, 1998.

[7] R. Molina, A. Katsaggelos, and J. Mateos, "Bayesian and resgularization methods for hyperparameter estimation in image restoration," *IEEE Transactions on Image Processing*, vol. 8, no. 2, pp. 231–246, 1999.

[8] O. Batu and M. Cetin, "Hyper-parameter selection in non-quadratic regularization-based radar image formation," *Proceedings of SPIE*, vol. 6970, 2008.

[9] J. Fienup, "Synthetic-aperture radar autofocus by maximizing sharpness," *Optics Letters*, vol. 25, no. 4, pp. 221–223, 2000.

[10] F. Berizzi and G. Corsini, "Autofocusing of inverse synthetic aperture radar images using contrast optimization," *IEEE Transactions on Aerospace and Electronic Systems*, vol. 32, no. 3, pp. 1185–1191, 1996.

[11] S. Fortune, M. Hayes, and P. Gough, "Statistical autofocus of synthetic aperture sonar images using image contrast optimisation," *Proceedings of OCEANS*, vol. 1, pp. 163–169, 2001.

[12] F. Ahmad, M. Amin, and G. Mandapati, "Autofocusing of through-the-wall radar imagery under unknown wall characteristics," *IEEE Transactions on Image Processing*, vol. 16, no. 7, pp. 1785–1795, 2007.

[13] M. Cetin, W. Karl, and D. Castanon, "Feature enhancement and ATR performance using nonquadratic optimization-based SAR imaging," *IEEE Transactions on Aerospace and Electronic Systems*, vol. 39, no. 4, pp. 1375–1395, 2003.

[14] "Mstar public targets." [Online]. Available: https://www.sdms.afrl.af.mil/datasets/mstar/targets.php

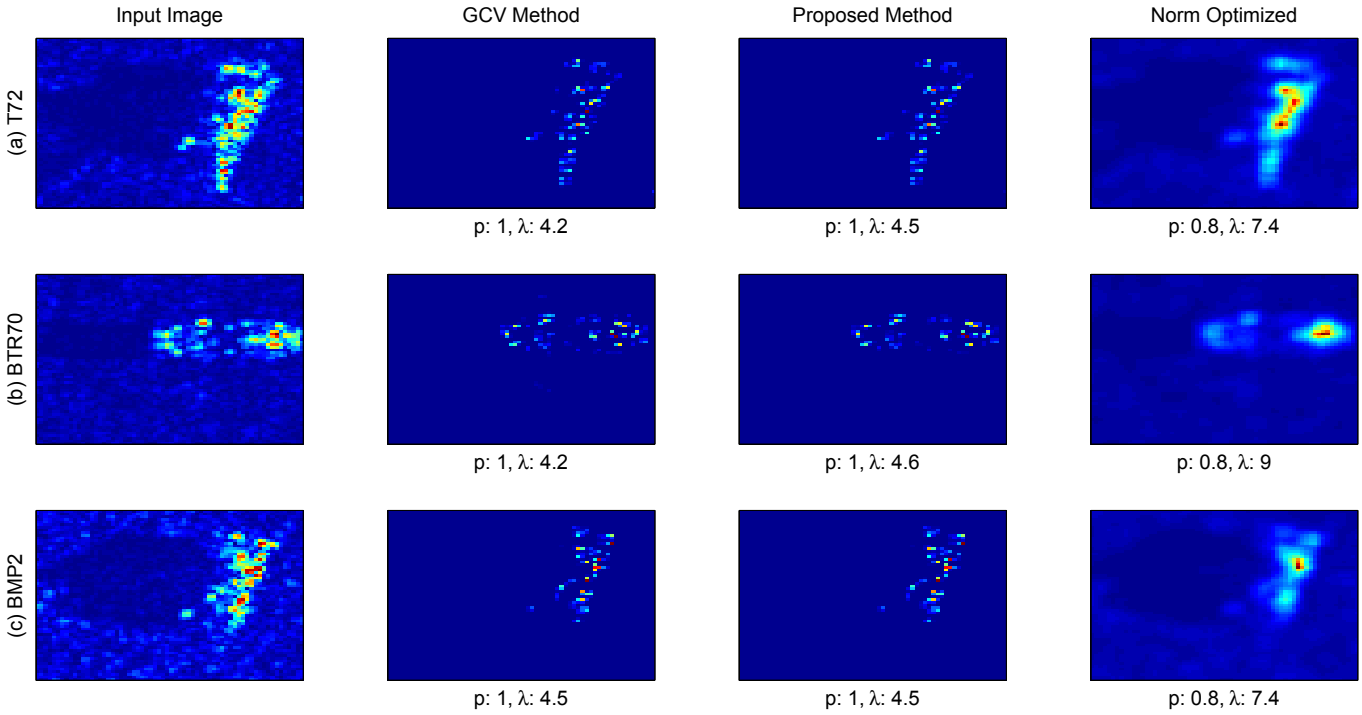

Fig. 4. Point-based enhancements showing original (top), reconstructed images with l_1-norm using GCV and gradient of kurtosis (middle), and norm optimized reconstructions (bottom).

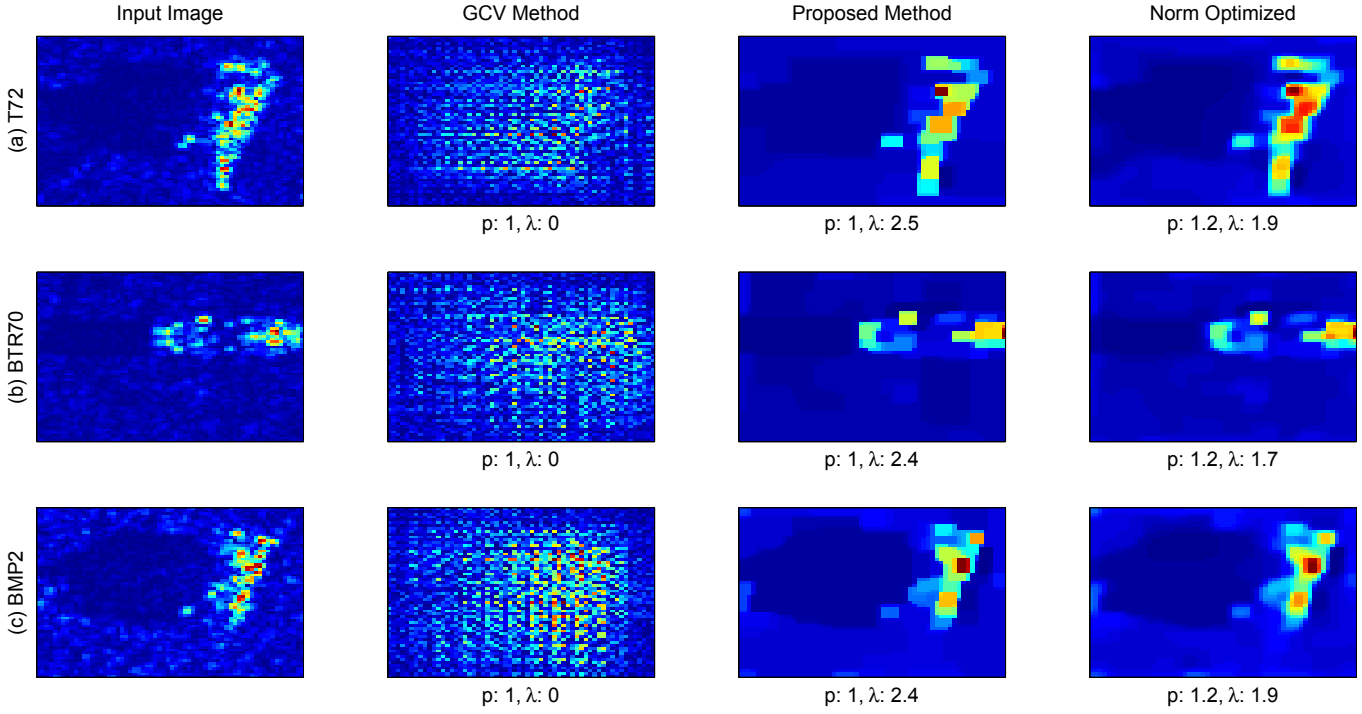

Fig. 5. Region-based enhancements showing original (top), reconstructed images with l_1-norm using GCV and gradient of kurtosis (middle), and norm optimized reconstructions (bottom).